JACS
JOURNAL OF THE AMERICAN CHEMICAL SOCIETY
Article
pubs.acs.org/JACS

Pressure Modulation of Ras–Membrane Interactions and Intervesicle Transfer

Shobhna Kapoor,[§] Alexander Werkmüller,[§] Roger S. Goody,[Δ] Herbert Waldmann,[‡,†] and Roland Winter*[,§]

[§]Physical Chemistry I—Biophysical Chemistry, Faculty of Chemistry, TU Dortmund University, Otto-Hahn-Strasse 6, D-44227 Dortmund, Germany

[Δ]Physical Biochemistry, Max Planck Institute of Molecular Physiology, Otto-Hahn-Strasse 11, D-44227 Dortmund, Germany

[‡]Department of Chemical Biology, Max Planck Institute of Molecular Physiology, Otto-Hahn-Strasse 11, D-44227 Dortmund, Germany

[†]Faculty of Chemistry, TU Dortmund University, Otto-Hahn-Strasse 6, D-44227 Dortmund, Germany

Supporting Information

ABSTRACT: Proteins attached to the plasma membrane frequently encounter mechanical stresses, including high hydrostatic pressure (HHP) stress. Signaling pathways involving membrane-associated small GTPases (e.g., Ras) have been identified as critical loci for pressure perturbation. However, the impact of mechanical stimuli on biological outputs is still largely *terra incognita*. The present study explores the effect of HHP on the membrane association, dissociation, and intervesicle transfer process of N-Ras by using a FRET-based assay to obtain the kinetic parameters and volumetric properties along the reaction path of these processes. Notably, membrane association is fostered upon pressurization. Conversely, depending on the nature and lateral organization of the lipid membrane, acceleration or retardation is observed for the dissociation step. In addition, HHP can be inferred as a positive regulator of N-Ras clustering, in particular in heterogeneous membranes. The susceptibility of membrane interaction to pressure raises the idea of a role of lipidated signaling molecules as mechanosensors, transducing mechanical stimuli to chemical signals by regulating their membrane binding and dissociation. Finally, our results provide first insights into the influence of pressure on membrane-associated Ras-controlled signaling events in organisms living under extreme environmental conditions such as those that are encountered in the deep sea and sub-seafloor environments, where pressures reach the kilobar (100 MPa) range.

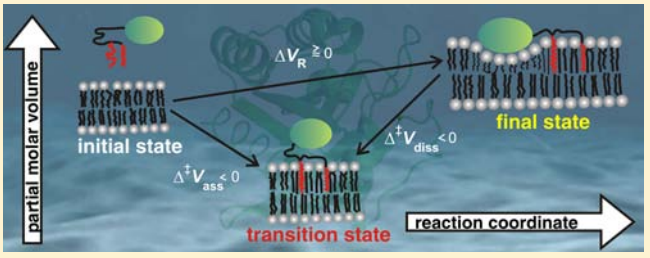

INTRODUCTION

The greatest portion of our biosphere on Earth is in the realm of environmental extremes, such as high hydrostatic pressure (HHP) and low temperature. The average pressure on the ocean floor is about 400 bar (40 MPa). Psychrophilic–barophilic (cold- and pressure-adapted) organisms are found even on the deepest ocean floor (at a depth of ∼11 000 m) and in deep-sea sediments where pressures up to about 1 kbar prevail.[1] The effect of HHP on structural–functional aspects of single biomolecules is quite well studied,[2−4] but its effect on membrane-associated processes remains largely unknown. Mechanical forces are known to be vital modulators of cellular processes, and transmembrane signaling events have been identified as important loci of pressure perturbation,[5,6] transduced by mechanosensitive biomolecules.[7−9] Mechanosensitivity has been largely elucidated for directional shear stress, but responsiveness toward nondirectional hydrostatic stress has also been reported.[5,10] Intriguingly, a key discovery in stress-signaling has been the activation of the MAPK/ERK pathway, of which Ras is a crucial nexus point.[6,10,11] Ras proteins are small GTPases that apically control the signaling pathways regulating cell proliferation and differentiation. They are plasma membrane localized molecular switches that function by shuttling between inactive GDP-bound and active GTP-bound forms.[11,12] Oncogenic Ras is a factor driving ∼30% of all human cancers.[12] Ras isoforms comprise N-, H-, and K-Ras that share an identical catalytic G-domain but differ at their C-terminus, known as the hypervariable region (HVR). The HVR houses divergent lipid-modified motifs that enable the isoforms to bind to distinct membrane domains.[13] Besides the biological relevance of pressure-dependent studies, the use of pressure as a kinetic and thermodynamic variable is also of significant biophysical relevance: non-covalent forces such as hydrophobic and electrostatic forces stabilize interactions in biomacromolecular assemblies, and the alteration of these weak interactions by pressure allows novel insights into the significance of such forces in biomolecular assembly and

Received: December 28, 2012
Published: April 5, 2013

   dx.doi.org/10.1021/ja312671j | J. Am. Chem. Soc. 2013, 135, 6149−6156

function.[2−4] In addition, pressure studies allow determination of activation and reaction volumes along the reaction path and hence provide additional mechanistic information.

Membrane fluidity—among the most pressure sensitive cellular properties—will be altered by pressure changes, and the fluidity change will in turn affect membrane functions such as permeability, ion transport, and signal transduction.[2] Pressure may affect signaling in various ways, e.g., by altering a protein's conformational substates, modifying the rate of ligand binding, and modifying the interaction with membranes, receptors, and other proteins.[14−16] In more general terms, pressure influences those membrane-associated processes most that are accompanied by large volume changes. HHP retards or fosters the interaction when the reaction volume is positive or negative, respectively. Contributors to negative volume changes, to mention a few, are release of the void volumes initially devoid of water (due to imperfect packing of two macromolecular surfaces), electrostriction, and lipid membrane condensation.[17−20] Volume changes accompanying interprotein associations are exhaustively studied, but those accompanying protein−membrane interactions are scarce.[21] Membrane properties, such as surface charge, hydration, curvature, packing density, and lateral organization, present the most prominent features influencing volume changes upon protein−membrane binding.[22] As the lipid headgroup is relatively incompressible compared to the lipid bilayer interior, application of pressure increases the packing density of lipid chains only. Thereby, the membrane thickness along the lipid chain increases, accompanied by a concomitant decrease in the cross-sectional lipid chain area.[23] Lateral heterogeneities (e.g., the coexistence of liquid-ordered/liquid-disordered (l_o/l_d) phases in raft-like membranes) in membranes have been demonstrated to have profound physiological implications on Ras−membrane interactions.[24−26] High pressure promotes chain ordering and is expected to steadily reduce the amount of fluid-like l_d phase in membranes upon pressurization, finally giving way to all-ordered phases at sufficiently high pressures.[22] Hence, pressure is expected to heavily modulate the membrane binding of lipidated proteins and requires thorough investigation, underscored by the evidence that the postsynthetic lipid modifications of proteins play a major role in membrane partitioning and stabilization via the classical hydrophobic effect,[26] which itself weakens upon pressurization.[19]

In this study, the effect of HHP on the membrane association, dissociation, and intervesicle transfer process of fully lipidated GDP-bound N-Ras HD/Far (hexadecyl/farnesyl) was explored, and the associated kinetic and volumetric changes were delineated. Different membrane compositions were used to reveal the role of lipid bilayer packing and heterogeneity. HHP was shown to foster the membrane association of N-Ras proteins, largely independent of the membrane composition. The dissociation reaction, on the other end, revealed a more tenuous membrane composition dependence under pressure. Activation volume-based analysis furnished insights into the physical properties of the transition and the final states of the Ras−membrane interaction process. Upon pressurization, the intermolecular interactions and reaction rates of biological assemblies are solely dominated by the volume changes of the various processes. Thus, pressure perturbed cellular signaling could lead to modulated signal outputs and kinetics, and improve our understanding of the precisely controlled signaling events also under extreme environmental conditions.

RESULTS AND DISCUSSION

Description of the Vesicle Transfer Model and Ambient Pressure Data. There are principally two distinct mechanisms conceivable for the transfer of a lipidated protein between lipid vesicles: (a) the aqueous diffusion model, i.e., the diffusion through the aqueous phase separating the membranes, and (b) the collision-mediated model, i.e., the transfer mediated by intervesicle collisions. At the relatively low lipid concentrations employed here, the collision-mediated model is not expected to play a significant role.[27−29] The rate equations describing the diffusion pathway (Figure 1A) for the Ras−

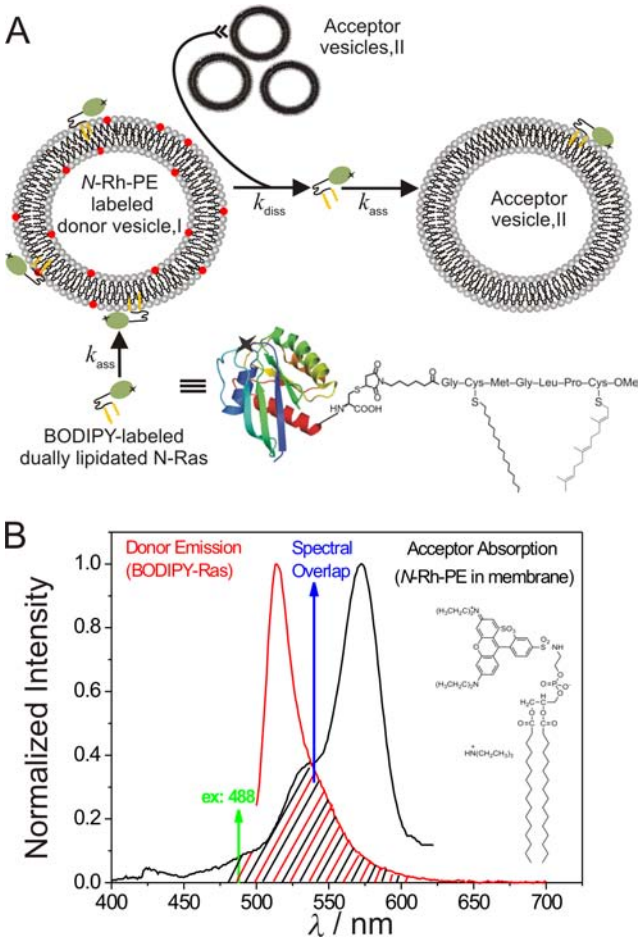

Figure 1. FRET-based assay for studying Ras−membrane interaction. (A) Schematic diagram of the diffusion-mediated transfer process. (B) Spectral characterization of the FRET pair used. The structure of the N-Ras G-domain was adopted from the PDB entry 4q21.

membrane interaction (with rate constants k_{ass} and k_{diss} for the association to and dissociation from the membrane) and the intervesicle transfer (with rate constant k_{trans}) have been formulated and explained in detail in the Supporting Information. Since in the absence of any collision-mediated transfer the rate-limiting step for the intervesicle transfer process is given by the dissociation of protein from the donor vesicles, and under the experimental conditions given, k_{diss} represents approximately the rate constant of vesicle transfer, i.e., $k_{trans} \approx k_{diss}$.

A significant overlap between the emission and absorption spectra of BODIPY and *N*-Rh-PE, which were used as fluorescence labels for the protein and membrane, respectively,

dx.doi.org/10.1021/ja312671j | J. Am. Chem. Soc. 2013, 135, 6149−6156

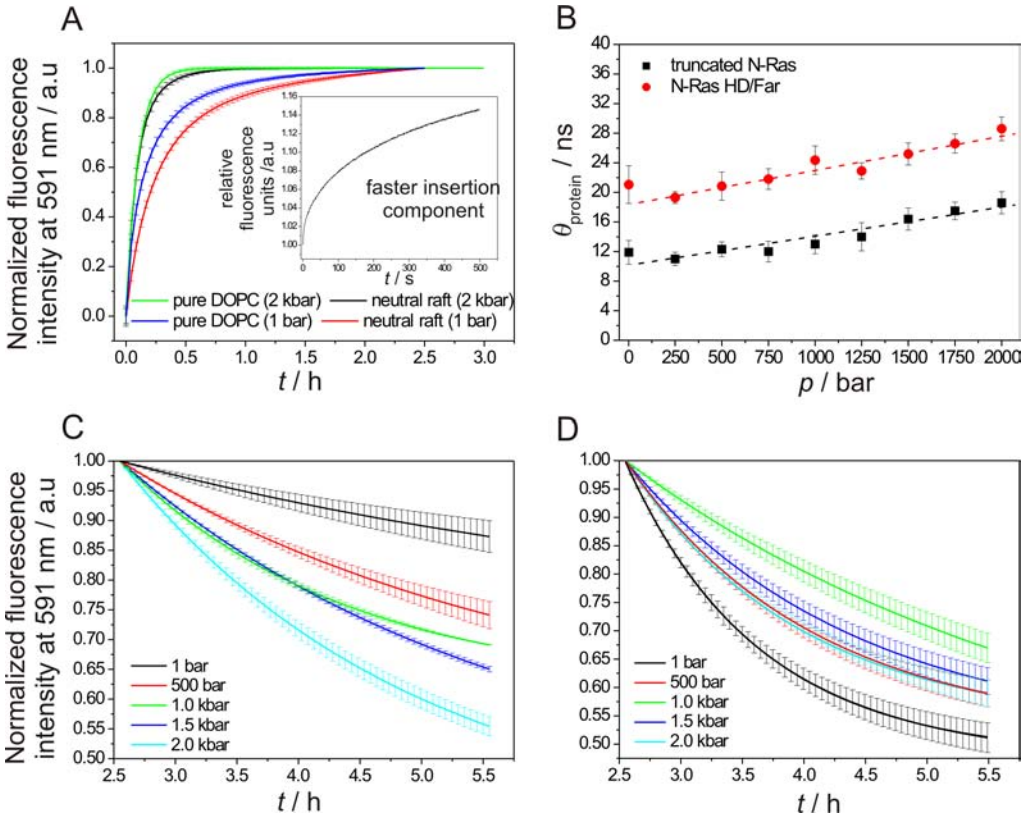

Figure 2. Effect of HHP on the kinetics of the N-Ras HD/Far−membrane interaction process. (A) Time-dependent increase in the normalized fluorescence intensity due to energy transfer from BODIPY-N-Ras to *N*-Rh-PE-labeled DOPC and the neutral raft-like (DOPC/DPPC/Chol 25:50:25 (molar ratio)) lipid vesicles upon addition of N-Ras to the vesicle solution. Inset: Stopped-flow assay depicting the fast insertion step of the labeled N-Ras (monitoring time <500 s) to the labeled DOPC vesicles at 1 bar; owing to the fast mixing process in the stopped-flow setup, the fast kinetic component is a factor of 10 faster, whereas the second, slower component is similar in magnitude to that measured in the high-pressure cell. (B) Pressure dependent rotational correlation time of BODIPY-labeled full-length and truncated N-Ras protein in solution; the lipidated N-Ras protein exists mainly as dimers in solution, revealed by a doubled rotational correlation time compared with the truncated protein, i.e., in the absence of the hypervariable region. Slight changes in the rotational correlation time with increasing pressure are due to the increase in solvent viscosity with pressure, in accordance with the Stokes−Einstein law. (C,D) Time-dependent decrease in the normalized fluorescence intensity, due to the loss of energy transfer from BODIPY-N-Ras to *N*-Rh-PE-labeled DOPC (C) and neutral raft lipid mixture (D) upon addition of the corresponding unlabeled lipid vesicles.

indicated energy transfer between the two fluorophores in close proximity (Figure 1B).[30] An increased emission from *N*-Rh-PE was observed at 591 nm (Figure S1−S3) following the addition of BODIPY-N-Ras into the solution and subsequent insertion into *N*-Rh-doped lipid vesicles. The recorded fluorescence intensity was corrected for the background intensities from donor and acceptor alone at different pressures, and best fits for the time-dependent fluorescence intensity changes were obtained with a biexponential function (Figures S3 and S4), representing the two steps for the insertion process: an initial docking, reorientation, and subsequently high-affinity insertion of N-Ras into the membrane mediated by its lipid anchors as the first step,[30] and a second step that embodies lateral reorganization and clustering of N-Ras within the membrane plane, as shown recently by atomic force microscopy (AFM) studies.[24,25] Figure 2A (blue and red) shows the biexponential fits for the N-Ras association to the DOPC and raft-like membrane at 1 bar (the inset exhibits the better time resolution for the fast association process into DOPC bilayers obtained from stopped-flow experiments). Tables S1−S3 display all kinetic rate constants.

The kinetics was measured in unstirred solution, i.e., a diffusion-limited component in bulk solution. Upon docking to the lipid membrane, significant activation energy barriers might be invoked, however, leading to an overall reaction-limited kind of process. As the kinetics depends on the concentration and sample geometry, the kinetic constants given here are effective rate constants. The first phase in the association curves with rate constants $k_{ass,1}$ = 10.1 and 4.8 h^{-1}—corresponding to half-lives of 4 and 8.6 min, respectively—are of the same order of magnitude in both membrane systems at ambient pressure, which is expected as N-Ras HD/Far is known, from AFM and fluorescence microscopy data, to partition initially into the fluid phase of the lipid membrane.[24−26] Minor differences in the initial association rate constants may be due to differences in lateral organization and lipid chain packing of the two membranes. Preferential insertion into the fluid phase is probably controlled by the bulky nature of the farnesyl (Far) group, due to its stronger hydrophobic mismatch with the longer lipid acyl chains of the bilayer. A previous NMR study showed that saturated lipid anchors of membrane-associated Ras undergo remarkable adaptations with respect to the hydrophobic thickness of membranes, rendering the Gibbs free energy for hydrophobic mismatch almost zero.[31] No such adaptation in chain length is possible for the Far group, however.

dx.doi.org/10.1021/ja312671j | *J. Am. Chem. Soc.* 2013, 135, 6149−6156

The second, slower association rate constant was found to be similar in both lipid membrane systems, suggesting that the time scales for lateral reorganization and clustering of the protein are of similar magnitude. The clustering of proteins into distinct membrane domains is of biological relevance, as it is expected to increase the association rates to other downstream proteins in the signaling pathways due to a boost in the effective concentration (reaction cross-section) in particular regions of the membrane, causing significant signal amplification.[32]

High Pressure Fosters Membrane Association of N-Ras. The association kinetics of N-Ras to the different lipid membranes were then measured at 2.0 kbar, a pressure still far below the unfolding pressure of Ras.[14] As a control, pressure effects on pure BODIPY-FL and *N*-Rh-labeled DOPC/raft-like lipid vesicles in solution were also determined (Figure S5) and were found to contribute less than 5% of the observed fluorescence signal. Remarkably, the association of N-Ras to both membrane systems was found to be accelerated under pressure (Figure 2A, green and black), i.e., exhibiting higher association rate constants by factors of 2−4. One reason for the higher observed association rates was first thought to arise from a pressure-induced dissociation of protein clusters in solution. In fact, N-Ras HD/Far has been shown to exist essentially as a dimer in solution (Figure 2B), probably via interaction of their HVR/lipid anchor regions. However, this possibility was ruled out since the rotational correlation times—being sensitive to changes in the radius of gyration of the rotating particle—did not decrease upon pressurization (Figure 2B). Another reason considered was the pressure-induced reversal of back-folding of the HVR onto the protein surface, since the HVR in Ras proteins does make contacts (i.e., is sequestered) to the G-domain (referred to as back-folding[33]), so that high pressures could reverse this effect and contribute to the higher association rates. However, owing to the weak interaction between the HVR and the G-domain and since the HVR remains fully hydrated, the required volume change for a pressure effect to be operative can be expected to be negligible. Other factors, such as an increase in protein number density and curvature or vesicle shape changes upon pressurization could also be ruled out: Owing to the small solution density change in the pressure range covered (<8%), the number density of the protein does not change markedly. Surface plasmon resonance (SPR)-based binding studies using lipid compositions with marked stored curvature elastic stress did not reveal a significant effect on the binding and dissociation processes of lipidated N-Ras, indicating insensitivity of the binding process to pressure-induced shape changes in the lipid vesicle—if there are any.[30,34]

At this stage, high-pressure mechanistic delineation based on activation volumes[14,15,35] was applied to characterize the transition state of the protein−membrane interaction process, and to attempt to uncover the underlying mechanistic principles. Determination of the activation volumes for the association and dissociation steps also permitted calculation of the overall reaction volume (ΔV_R), and provided a glimpse of the structural properties of the final proteolipid system. Measurement of the pressure dependence of the effective association rate constant, $k_{ass,1}$, at a temperature T enabled the calculation of the activation volume, $\Delta^{\ddagger}V_{ass}$, for the association process. $\Delta^{\ddagger}V_{ass}$ values for the insertion of N-Ras into DOPC and raft-like membranes were found to be -7.1 ± 0.2 and -17.0 ± 1.8 cm^3 mol^{-1}, respectively. The volume profiles for the association process exhibiting negative values for the transition state indicate a compact transition state with a reduced overall volume. Differences between the two membrane systems are probably due to differences in the packing properties and hence free volumes of the different lipid systems.[36] A higher acyl chain ordering and tighter packing of the lipid chains induced by high pressure is invariably accompanied by a reduction in volume.[37] For comparison, the pressure-induced increase of the packing density in a lipid bilayer upon a pressure-induced phase transition from the fluid to the ordered gel state is accompanied by a volume reduction of ∼−30 cm^3 mol^{-1}. Assuming a volume change of similar magnitude to contribute to the decrease in activation volume, an 11-fold increase in the rate constant would be expected at ∼2 kbar. Increased van der Waals interactions between the lipid acyl chains and the protein's lipid anchors, coupled with the decrease of conformational space in the lipid anchor region and HVR upon membrane insertion are expected to favor membrane partitioning of the lipidated protein due to an overall volume decrease at high pressures, hence favoring formation of a compact proteolipid transition state.

Differences in the activation volumes of the different membrane systems are expected to arise from the respective volume fluctuations in the two lipid bilayer systems.[38] The phase boundary regions in the raft-like membranes are associated with higher area and volume fluctuations; hence, a larger reduction in the free volume is expected upon pressurization.

Pressure Affects Dissociation of N-Ras in a Membrane-Dependent Manner. Intervesicle N-Ras transfer was initiated by adding an 8-fold excess of unlabeled lipid vesicles (acceptor vesicles) of the same size and composition to the Ras-bound fluorescently labeled vesicles (donor vesicles) once a stable baseline was reached in the association process. Such transfer experiments have already been shown as appropriate models to obtain kinetic details for the transfer of lipidated peptides under ambient pressure conditions.[38] The observed time-dependent decrease in the Förster resonance energy transfer (FRET) signal results from the transfer of the BODIPY-labeled N-Ras from the donor to acceptor vesicles. The time-dependent fluorescence intensity recorded at each pressure was corrected by subtracting the respective associated fluorescence signal from BODIPY-N-Ras, the cross excitation intensity from *N*-Rh-PE-labeled donor vesicles, and any from the unlabeled acceptor vesicles. The intensity profile was then analyzed by curve-fitting to an equation of the form $F = A + B \exp(-k_{diss}t)$, where k_{diss} is the apparent rate constant of the protein dissociation process, which corresponds to the rate of vesicle transfer ($k_{diss} \approx k_{trans}$), as explained above.

Figure 2C exhibits kinetic curves for the dissociation process of N-Ras from the fluid DOPC membrane at different pressures. The associated $k_{diss}(p)$ data are given in Table S2. The first-order dissociation rate constant at 1 bar corresponds to a long half-life ($t_{1/2}$) of ∼3.6 h—as expected for a stably inserted dually lipidated protein. The high binding stability imparted by a second lipid anchor drastically slows down the rate of spontaneous intermembrane transfer.[39] At 2 kbar, the protein shows a somewhat greater but still very slow dissociation rate with $t_{1/2} \approx 1.6$ h. The corresponding transfer rate of the N-Ras peptide sequence alone is 3.7×10^{-2} h^{-1} at ambient pressure, corresponding to $t_{1/2} \approx 19$ h.[39] The higher dissociation rate observed for the full length protein in this study may be attributed to a regain of configurational, translational, and rotational entropy upon transfer into the

dx.doi.org/10.1021/ja312671j | J. Am. Chem. Soc. 2013, 135, 6149−6156

aqueous phase, which is lost when the lipidated protein binds to the membrane. In fact, this effect has been predicted to increase the spontaneous intervesicle transfer rate of the full-length lipidated protein by typically 5- to 10-fold compared with the corresponding peptide construct.[39]

The dissociation and hence (spontaneous) intervesicle transfer rate of N-Ras from the DOPC membrane increases upon pressurization (Figure 2C), which can be accounted for by the nature of the fluid lipid bilayer system: The pure fluid DOPC membrane does not exhibit any phase transition to a gel-like or solid-ordered (s_o) phase in the pressure−temperature phase space covered here.[1] Even at a pressure of 2 kbar, the DOPC bilayer is still in the fluid phase, but exhibits an overall slightly higher packing density due to pressure-induced acyl chain ordering.[1] Upon pressurization, no stable protein−membrane anchorage is maintained. Conversely, pressure-induced lipid chain ordering induces higher membrane association rates of N-Ras. It may be expected that the saturated HD and the unsaturated Far lipid anchors serve as mutually exclusive sensors of the pressure-induced membrane ordering. Whereas higher rates of association may be tackled by the increased (though transient) stabilization of the HD anchor within the ordered membrane, higher rates of dissociation may be controlled by the bulky Far anchor. The latter effect may be markedly enhanced in the case of lateral clustering of N-Ras proteins, which is expected to precede the dissociation step. Differences in the orientation and hence interaction of the HVR of N-Ras might be a further stability determinant for the membrane anchorage. The activation volume for the dissociation step, $\Delta^{\ddagger}V_{diss}$, in the DOPC membrane was calculated to be -9.7 ± 0.7 cm^3 mol^{-1}. Combined with the $\Delta^{\ddagger}V_{ass}$ value for the association process, a tentative volume profile for this reaction could be obtained, which is depicted in Figure 3. From Figure 3 it is clear that the final proteolipid system rearranges, increasing its volume en route from the transition state. One possible reason mediating this effect could be the interaction of the G-protein and its HVR with the lipid interface, hence perturbing the lipid bilayer, particularly in the clustered state, thereby inducing lateral expansion and thinning

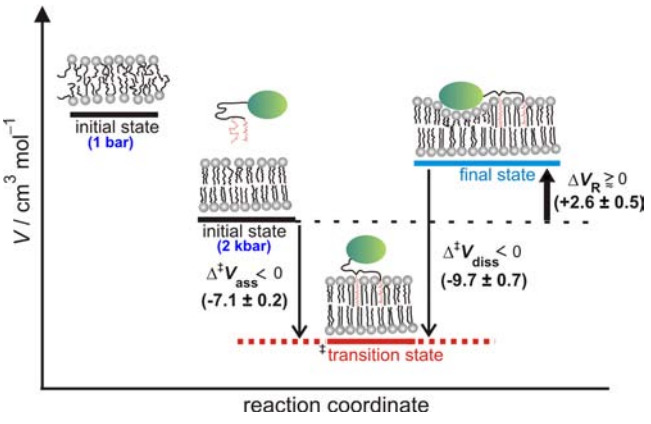

Figure 3. Volume profile for the interaction between N-Ras HD/Far and a pure fluid membrane. The ordinate shows the relative changes in the volume of the proteolipid system and the abscissa delineates the reaction coordinate for the interaction process. Schematic representation of the structures of the initial states of the membrane at ambient and high pressures, the suggested structures of the relatively compact transition state, and the relaxed final state of the interaction are depicted.

(indentation) of the membrane.[40] A schematic view of such a hypothetical scenario is depicted in Figure 3.

Similar intervesicle transfer studies were carried out with the neutral heterogeneous membrane. These bilayer membranes can be envisioned as platforms of l_o domains dispersed in a fluid l_d matrix of mostly unsaturated lipids. The l_o domains are more ordered and tightly packed, but they are still rather mobile, mainly due to lipid packing differences.[30] Phase separation in such heterogeneous membranes creates a unique compositional phase boundary, where membrane properties change rather abruptly and exhibit high area and volume fluctuations.[36] To N-Ras, such domain boundaries have been shown by recent AFM data to represent "hot spots", where N-Ras partitioning takes place, thereby decreasing the unfavorable line energy between domains and stabilizing the interfaces, which leads to weaker repulsive interactions between the membrane domains.[26] The still partial fluid character of these membranes enables them to respond rapidly to an incoming (mechanical) stimulus, through the formation or dissipation of structurally and compositionally distinct lipid domains, which, by virtue of the lipid's nearest neighbor contacts, allow the changes to be rapidly communicated and a cooperative response to follow. Upon pressurization, the amount of l_o domains increases at the expense of fluid lipid assemblies.[1,20] Such effect may be expected to modulate the intervesicle transfer rate of the N-Ras protein as well.

In contrast to the fluid DOPC membrane, the spontaneous rate of N-Ras intervesicle transfer with raft-like membranes decreases under pressure, by almost an order of magnitude (Figure 2D). The first-order rate constant for the dissociation process corresponds to $t_{1/2} \approx 1$ h at ambient pressure. This value is similar to that obtained at 2 kbar in the pure fluid DOPC membrane, suggesting that the pressure-induced ordering in the DOPC membranes at ∼2 kbar closely resembles the average degree of ordering prevalent in the heterogeneous membranes under ambient pressure conditions. The coexistence of l_o and l_d domains, with a certain percentage of saturated lipids and cholesterol also within the l_d phase, in heterogeneous membranes account for a higher degree of order.[30] The transfer rates upon pressurization exhibit substantial changes at ∼1 kbar, which may be correlated with a phase-transition occurring for this membrane composition.[20] The $p-T$ phase diagram of this lipid mixture displays a transformation from an l_d+l_o two-phase region to a more ordered l_d+l_o+s_o three-phase region in this pressure range. The s_o phase exhibits a gel-like, highly ordered (*all-trans*) acyl chain configuration, which is not likely to provide a suitable environment for the lipid anchors of Ras. In fact, the phase sequence for preferential binding of N-Ras in heterogeneous membranes was shown by SPR binding studies to be in the order $l_d > l_o \gg s_o$.[41] In addition, an increase of pressure leads to a steady reduction in the amount of l_d phase. N-Ras still prefers to partition into the reduced l_d domains, which, by virtue of their small sizes (at high pressures), drastically increases the local N-Ras concentration. The spatial constraints imposed on the N-Ras proteins, in turn, are expected to induce reorientational and conformational changes and finally clustering within the membrane plane. Increased protein contacts might stabilize the protein clusters, thereby conferring a reduced dissociation rate at high-pressure conditions, coupled with a higher activation volume required for membrane desorption in the clustered state. In fact, such a scenario is in line with experimental observations.[42] The activation volume for dissociation, $\Delta^{\ddagger}V_{diss}$, of the N-Ras protein from raft-like

dx.doi.org/10.1021/ja312671j | J. Am. Chem. Soc. 2013, 135, 6149−6156

heterogeneous membranes was calculated to be 4.3 ± 0.5 cm^3 mol^{-1}. Combining this value with the activation volume of association, a volume profile for its interaction with the heterogeneous membrane could be obtained, displaying a reaction volume of −20.9 ± 2.4 cm^3 mol^{-1} (Figure 4). The final

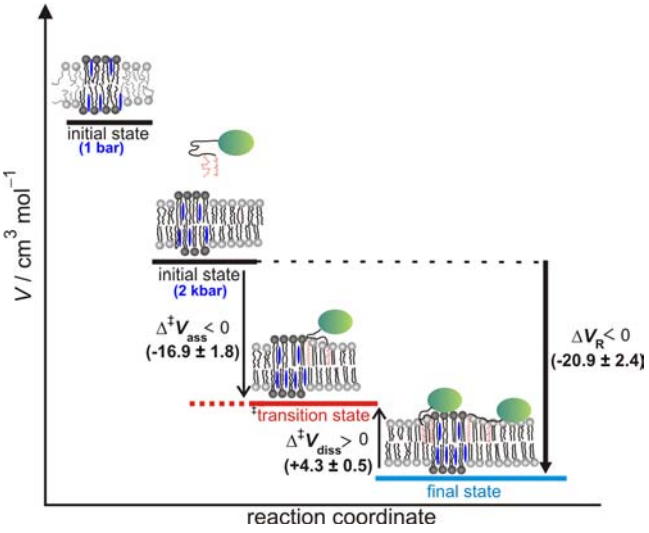

Figure 4. Volume profile for the interaction between N-Ras HD/Far and a raft-like membrane. The ordinate shows the relative changes in the volume of the proteolipid system, and the abscissa delineates the reaction coordinate for the interaction/insertion process. Schematic representations of the structures of the initial states of the raft-like membrane at ambient and high pressures, the suggested structures of the relatively compact transition state, and the compact final state of the interaction are depicted.

state of the heterogeneous membrane-bound N-Ras exhibits an overall smaller volume compared with the initial state, probably due to the preferential insertion of the protein at the phase boundary of lipid domains, thereby reducing the free volume of the lipid system. The volume is probably further reduced under higher pressure due to an increased clustering mediated by the decreasing amount of l_d phase. Hence, membrane composition and lateral organization seem to significantly influence the pressure effect on membrane dissociation of N-Ras.

■ CONCLUSIONS

Adaptation of proteins to external chemical and physical stimuli is of utmost importance in maintaining the cycle of life. Ras proteins attached to the plasma membrane frequently encounter mechanical stresses, from extensive actin mesh-like structures, hemodynamic flow, up to high hydrostatic pressure (HHP) stresses. The present study explores the effect of HHP on a membrane-associated signaling module, specifically Ras−membrane association, dissociation, and spontaneous intervesicle transfer, to reveal the associated kinetic and volumetric parameters underlying the membrane partitioning and intervesicle transport process. FRET-based assays reveal a biphasic nature of Ras membrane binding, where the first step is most likely the initial docking, reorientation, and subsequent high-affinity insertion of the protein into the membranes. The second step stems from a lateral reorganization of Ras proteins, which eventually leads to cluster formation as confirmed by AFM data.[24,25]

The use of lipid membranes of different composition and lateral organization resulted in only minor differences in the association rate constants. Notably, HHP fosters association of the dually lipidated N-Ras protein to lipid membranes, independent of the lipid composition. Calculation of the activation volumes for the association process revealed a highly compact transition state with reduced overall volume, essentially originating from changes in the free volume of the different lipid membranes.

The dissociation process, both under ambient and high-pressure conditions, displayed differences in a membrane-dependent manner. The dissociation rate of N-Ras is increased in pure homogeneous fluid membranes and the concomitant volume profile reveals a rearrangement of the final lipoprotein system encompassing lateral expansion and thinning of the lipid membrane due to the interaction and perturbation of the membrane with N-Ras and its HVR, eventually increasing the system's volume en route from the transition state. In contrast, for the heterogeneous raft-like membrane, a retardation of the dissociation step was affirmed. The calculated activation volume for this step revealed that the final system is even more compact than the transition state, owing to a deep free energy minimum for heterogeneous membrane-bound N-Ras, where partitioning at the domain boundary decreases the unfavorable line energy and diminishes the repulsive forces between the adjoining domains. In addition, HHP can be inferred as a positive regulator of N-Ras clustering (due to decreasing amounts of l_d phase) especially in heterogeneous membranes, imposing intermolecular constraints on N-Ras orientation and enhanced clustering, leading to retardation in the dissociation rates.

Taken together, these studies provide evidence that the N-Ras lipid anchors serve as mutually exclusive sensors of the pressure-induced ordering in membranes. The susceptibility of membrane interaction to pressure raises the idea of a role of lipidated signaling molecules as mechanosensors, thereby transducing mechanical stimuli to chemical signals by regulating their membrane binding and dissociation. In fact, as the lateral compressibility of lipid membranes is among the highest compressibilities found among biomolecular systems (for example, the cross-sectional area of fluid DPPC molecules changes by about −10 $Å^2$/kbar),[46] and as we know that the lateral pressure profile of lipid membranes is able to modulate membrane protein function,[47] we might speculate that the mechanosensitivity of membrane-associated processes is in fact a general phenomenon.

The stabilization of the long saturated lipid anchor within the ordered membrane is reflected in higher association rates to the membranes, but the higher rates of intervesicle transfer may be controlled by the bulky unsaturated lipid anchor of N-Ras and the tendency toward clustering in a membrane dependent manner. The composition and edifice of lipid membranes strongly regulates their interaction with N-Ras and probably other lipidated proteins as well as their partitioning behavior.

Finally, these results also shed light on the effect of pressure on membrane-associated Ras-controlled signaling events under extreme environmental conditions. Although pressure is an important environmental parameter, such as in the deep sea where organisms have to cope with pressures up to the 1 kbar range, the fundamental understanding of its effects remains largely unknown. Despite the fact that membranes are among the most pressure-sensitive biomolecular assemblies, the effects of pressure on the dynamics of signaling processes remain largely unexplored on a molecular level. Our data indicate that increased hydrostatic pressure may—in a membrane-dependent manner—markedly foster or retard kinetic events

dx.doi.org/10.1021/ja312671j | J. Am. Chem. Soc. 2013, 135, 6149−6156

associated with the partitioning of lipidated signaling proteins into membranes, and is hence expected to modulate the interaction with membrane-associated downstream interaction partners.

EXPERMENTAL SECTION

Materials and Sample Preparation. The phospholipids 1,2-dioleoyl-*sn*-glycero-3-phosphocholine (DOPC) and 1,2-dipalmitoyl-*sn*-glycero-3-phosphocholine (DPPC) were purchased from Avanti Polar Lipids (Alabaster, AL), cholesterol (Chol) from Sigma-Aldrich. All other reagents and solvents were obtained from Sigma-Aldrich and Merck. Stock solutions of 10 mg mL^{-1} lipids (DOPC, DPPC, and Chol) in chloroform (Merck, Darmstadt, Germany) were prepared and mixed to obtain the desired composition of the DOPC/DPPC/Chol (1:2:1 molar ratio) lipid mixture. The majority of the chloroform was evaporated with a nitrogen stream; all remaining solvent was subsequently removed by drying under vacuum overnight. The fluorescent lipid *N*-(lissaminerhodamine B sulfonyl)-1,2-dihexadecanoyl-*sn*-glycero-3-phosphoethanolamine triethylammonium salt (*N*-Rh-DHPE) and BODIPY-FL were from Molecular Probes (Invitrogen).

Synthesis of the Dually Lipidated N-Ras (N-Ras HD/Far). The synthesis of post-translationally modified N-Ras proteins was accomplished using maleimidocaproyl (MIC)-controlled ligation as described before.[43−45] Briefly, the N-Ras protein was expressed in a truncated form in *E. coli* with a free C-terminal cysteine required for the ligation. The truncated protein was ligated to the C-terminal prenylated maleimido peptide sequence, generated via Fmoc chemistry. The labile acyl thioester of the palmitoyl lipid group was replaced by a stable hexadecylthioether to prevent spontaneous decomposition of the palmitate group. BODIPY labeling of the protein core (at the N-terminus of the protein) was accomplished (before the ligation step) by mixing with 10-fold excess of BODIPY-NHS. The labeled protein was purified using a Hi-Trap desalting column and concentrated.

High-Pressure Fluorescence Spectroscopy and Anisotropy. All fluorescence spectroscopy and anisotropy measurements were performed on a K2 multifrequency phase and modulation fluorometer coupled with a stainless steel high-pressure vessel (ISS, Champaign, IL).The FRET-based studies were performed using *N*-Rh-PE-labeled lipid vesicles as the *acceptor*. BODIPY-labeled N-Ras HD/Far was used as *donor*, with a molar ratio of *N*-Rh-PE to BODIPY of 2:1 and a protein to lipid molar ratio of 1:360. The dissociation process was initiated by adding an 8-fold molar access of unlabeled lipid vesicles to the fluorescent protein-bound labeled vesicles. Excitation light of 488 nm was provided by a xenon lamp through a monochromator. Single point emission intensity at 591 nm was collected at 90° through a second monochromator. The mixed protein−lipid solution was injected into a spherical quartz cell (volume 0.8 mL) and sealed with an O-ring. The cell was then placed in the high-pressure vessel equipped with two quartz windows and connected to a pressure pump and gauge. High-quality (18 MΩ) water was used as pressurizing medium. The high-pressure cell was connected to a water bath maintained at 25 °C. Closure of the high-pressure cell and application of pressures (>1 kbar) resulted in a time delay of several minutes before collecting the fluorescence signal. Measurement of the pressure dependence of the rate constants, k, for the association or dissociation process, at temperature T, enabled calculation of the corresponding activation volumes:

$$\Delta^{\ddagger}V_{\mathrm{ass/diss}} = -RT\left(\frac{\partial \ln(k_{\mathrm{ass/diss}})}{\partial p}\right)_T = \left(\frac{\partial \Delta^{\ddagger}G_{\mathrm{ass/diss}}}{\partial p}\right)_T \quad (1)$$

where $\Delta^{\ddagger}V_{\mathrm{ass/diss}}$ is the difference between the partial volumes of the transition state associated with the membrane interaction step, and that of the initial reactants (lipid and proteins) or the final proteolipid system, respectively.

Approximate rate equations for the interaction between BODIPY-labeled lipidated N-Ras protein (serving as the FRET donor) in vesicles I with *N*-Rh-PE doped lipid vesicles II (serving as the FRET acceptor) can be deduced assuming that (i) the rate at which a lipidated protein (P) dissociates from the surface of the lipid vesicle (off-rate) is proportional to its surface concentration on that vesicle, and (ii) the association rate (on-rate) is proportional to the product of its concentration (c_P) in the bulk solution and the external (outer) surface area of the vesicle (for details, see the SI). If the donor and acceptor vesicles are of the same composition, and the acceptor vesicle concentration is largely in excess of the donor, one yields for the time-dependent dissociation of the lipidated protein molecules[27]

$$c_{P,I}(t) = c_{P,I}(0)\, e^{-k_{P,I}^{-}t} \quad \text{or}$$

$$c_{P,II}(t) = c_{P,I}(0)(1 - e^{-k_{P,I}^{-}t}) \quad (2)$$

Hence, from the decay of the fluorescence intensity with time, $F(t)$, the dissociation or off-rate $k_{P,I}^{-} = k_{diss}$ can be calculated. The corresponding half-time for reaching equilibrium amounts to $t_{1/2} = \ln 2/k_{P,I}^{-}$. Under these experimental conditions, the rate of dissociation is directly related to the rate k_{trans} at which N-Ras transfers from the *N*-Rh-PE doped donor vesicles to the unlabeled acceptor vesicles. The initial association rate, $k_{P,I}^{+}$, can be measured by adding protein molecules at concentration $c_{P,free}$ to the bulk solution containing fluorescent-labeled lipid vesicles (population I). If $c_{P,I} = 0$ for $t = 0$, one obtains for the initial association process

$$c_{P,I}(t) = c_{P,free}(0)(1 - e^{-k_{ass,1}t}) \quad (3)$$

where $k_{ass,1}$ can be treated as an observed effective association rate constant, which can be determined from the time-dependent increase of the fluorescence intensity upon incorporation of BODIPY-labeled protein into the *N*-Rh-PE doped lipid vesicles due to the FRET between the respective fluorophores (for details, see SI).

For the anisotropy measurements, BODIPY-labeled full-length or truncated N-Ras (0.5 μM) was excited by use of a 473 nm laser diode directly connected to a function generator, yielding modulated excitation light over a frequency range of 2−131 MHz at a cross-correlation frequency of 400 Hz. The BODIPY emission was collected through a 505 nm long-pass filter. Fluorescence lifetime measurements were carried out at magic-angle conditions prior to the anisotropy experiments. Phase and modulation data were recorded at 25 °C, in 250 bar steps ranging from 1 to 2000 bar. Experimental data were fitted with the VINCI-Analysis software (ISS, Champaign, Il) to yield fluorescence lifetimes and rotational correlation times (for details, see SI).

ASSOCIATED CONTENT

Supporting Information

Details on the high-pressure fluorescence spectroscopy and anisotropy experiments; description of the transfer model and definition of the rate constants; Figures S1−S6 and Tables S1−S6 as described in the text. This material is available free of charge via the Internet at http://pubs.acs.org.

AUTHOR INFORMATION

Corresponding Author

roland.winter@tu-dortmund.de

Notes

The authors declare no competing financial interest.

ACKNOWLEDGMENTS

R.W. thanks the DFG and the International Max Planck Research School in Chemical Biology, Dortmund, for financial support.

REFERENCES

(1) Winter, R.; Lopes, D.; Grudzielanek, S.; Vogtt, K. *J. Non-Equilib. Thermodyn.* **2007**, *32*, 41−97.

(2) Silva, J. L; Foguel, D.; Royer, C. A. *Trends Biochem. Sci.* **2001**, *26*, 612−618.
(3) Mishra, R.; Winter, R. *Angew. Chem., Int. Ed.* **2008**, *47*, 6518−6521.
(4) Wu, H. J.; Zhang, Z. Q.; Yu, B.; Liu, S.; Qin, K. R.; Zhu, L. *Cell Physiol. Biochem.* **2010**, *26*, 273−280.
(5) Salvador-Silva, M.; Aoi, S.; Parker, A.; Yang, P.; Pecen, P.; Hernandez, M. R. *Glia* **2004**, *45*, 364−377.
(6) Paoletti, P.; Ascher, P. *Neuron* **1994**, *13*, 645−655.
(7) Gudi, S.; Nolan, J. P.; Frangos, J. A. *Proc. Natl. Acad. Sci. U.S.A.* **1998**, *95*, 2515−2519.
(8) Ferraro, J. T.; Daneshmand, M.; Bizios, R.; Rizzo, V. *Am. J. Physiol. Cell Physiol.* **2004**, *286*, C831−839.
(9) Li, Y. S.; Shyy, J. Y.; Li, S.; Lee, J.; Su, B.; Karin, M.; Chien, S. *Mol. Cell. Biol.* **1996**, *16*, 5947−5954.
(10) Tzima, E. *Circ. Res.* **2006**, *98*, 176−185.
(11) Wittinghofer, A.; Pai, E. F. *Trends Biochem. Sci.* **1991**, *16*, 382−387.
(12) Karnoub, A. E.; Weinberg, R. A. *Nat. Rev. Mol. Cell. Biol.* **2008**, *9*, 517−531.
(13) Rocks, O.; Peyker, A.; Bastiaens, P. I. *Curr. Opin. Cell Biol.* **2006**, *18*, 351−357.
(14) Kapoor, S.; Triola, G.; Vetter, I. R.; Erlkamp, M.; Waldmann, H.; Winter, R. *Proc. Natl. Acad. Sci. U.S.A.* **2012**, *109*, 460−465.
(15) Akasaka, K. *Chem. Rev.* **2006**, *106*, 1814−1835.
(16) Siebenaller, J. F.; Garrett, D. J. *Comp. Biochem. Physiol. Part B* **2002**, *131*, 675−694.
(17) Roche, J.; Caro, J. A.; Norberto, D. R.; Barthe, P.; Roumestand, C.; Schlessman, J. L.; Garcia, A. E.; García-Moreno, E.; Royer, B. C. A. *Proc. Natl. Acad. Sci. U.S.A.* **2012**, *109*, 6945−6950.
(18) Chalikian, T. V.; Macgregor, R. B., Jr. *J. Mol. Biol.* **2009**, *394*, 834−842.
(19) Hummer, G.; Garde, S.; Garcia, A. E.; Paulaitis, M. E.; Pratt, L. R. *Proc. Natl. Acad. Sci. U.S.A.* **1998**, *95*, 1552−1555.
(20) Weber, G.; Drickamer, H. G. *Q. Rev. Biophys.* **1983**, *16*, 89−112.
(21) Ernst, R. R. *Biochim. Biophys. Acta* **2002**, *1585*, 1−2.
(22) Winter, R.; Jeworrek, C. *Soft Matter* **2009**, *5*, 3157−3173.
(23) Eisenblätter, J.; Winter, R. *Biophys. J.* **2006**, *90*, 956−966.
(24) Weise, K.; Triola, G.; Brunsveld, L.; Waldmann, H.; Winter, R. *J. Am. Chem. Soc.* **2009**, *131*, 1557−1564.
(25) Weise, K.; Kapoor, S.; Denter, C.; Nikolaus, J.; Opitz, N.; Koch, S.; Triola, G.; Herrmann, A.; Waldmann, H.; Winter, R. *J. Am. Chem. Soc.* **2011**, *133*, 880−887.
(26) Weise, K.; Huster, D.; Kapoor, S.; Triola, G.; Waldmann, H.; Winter, R. *Faraday Discuss.* **2013**, *161*, 549−561.
(27) Nichols, J. W.; Pagano, R. E. *Biochemistry* **1982**, *21*, 1720−1726.
(28) Wimley, W. C.; Thompson, T. E. *Biochemistry* **1991**, *30*, 1702−1709.
(29) Nichols, J. W. *Biochemistry* **1988**, *27*, 1889−1896.
(30) Gohlke, A.; Triola, G.; Waldmann, H.; Winter, R. *Biophys. J.* **2010**, *98*, 2226−2235.
(31) Vogel, A.; Reuther, G.; Weise, K.; Triola, G.; Nikolaus, J.; Tan, K. K.; Nowak, C.; Herrmann, A.; Waldmann, H.; Winter, R.; Huster, D. *Angew. Chem., Int. Ed.* **2009**, *48*, 8784−8787.
(32) Parton, R. G.; Hancock, J. F. *Trends Cell. Biol.* **2004**, *14*, 141−147.
(33) Thapar, R.; Williams, J. G.; Campbell, S. L. *J. Mol. Biol.* **2004**, *343*, 1391−1408.
(34) Nicolini, C.; Celli, A.; Gratton, E.; Winter, R. *Biophys. J.* **2006**, *91*, 2936−2942.
(35) Benz, R.; Conti, F. *Biophys. J.* **1986**, *50*, 91−98.
(36) Kupiainen, M.; Falck, E.; Ollila, S.; Niemelä, P.; Gurtovenko, A. A.; Hyvönen, M. T.; Patra, M.; Karttunen, M.; Vattulainen, I. *J. Comput. Theor. Nanosci.* **2005**, *2*, 401−413.
(37) Böttner, M.; Ceh, D.; Jacobs, U.; Winter, R. *Z. Phys. Chem.* **1994**, *184*, 205−218.
(38) Silvius, J. R.; l'Heureux, F. *Biochemistry* **1994**, *33*, 3014−3022.
(39) Schroeder, H.; Leventis, R.; Rex, S.; Schelhaas, M.; Nägele, E.; Waldmann, H.; Silvius, J. R. *Biochemistry* **1997**, *36*, 13102−13109.
(40) Mesquita, R. M.; Melo, E.; Thompson, T. E.; Vaz, W. L. *Biophys. J.* **2000**, *78*, 3019−3025.
(41) Nicolini, C.; Baranski, J.; Schlummer, S.; Palomo, J.; Lumbierres-Burgues, M.; Kahms, M.; Kuhlmann, J.; Sanchez, S.; Gratton, E.; Waldmann, H.; Winter, R. *J. Am. Chem. Soc.* **2006**, *128*, 192−201.
(42) Bhagatji, P.; Leventis, R.; Rich, R.; Lin, C. J.; Silvius, J. R. *Biophys. J.* **2010**, *99*, 3327−3335.
(43) Kuhn, K.; Owen, D. J.; Bader, B.; Wittinghofer, A.; Kuhlmann, J.; Waldmann, H. *J. Am. Chem. Soc.* **2001**, *123*, 1023−1035.
(44) Schelhaas, M.; Glomsda, S.; Hänsler, M.; Jakubke, H. D.; Waldmann, H. *Angew. Chem., Int. Ed.* **1996**, *35*, 106−109.
(45) Nägele, E.; Schelhaas, M.; Kuder, N.; Waldmann, H. *J. Am. Chem. Soc.* **1998**, *120*, 6889−6902.
(46) Eisenblätter, J.; Winter, R. *Z. Phys. Chem.* **2005**, *219*, 1321−1345.
(47) Jensen, M. Ø.; Mouritsen, O. G. *Biochim. Biophys. Acta* **2004**, *1666*, 205−226.